

# Analyst

Accepted Manuscript



This is an *Accepted Manuscript*, which has been through the Royal Society of Chemistry peer review process and has been accepted for publication.

*Accepted Manuscripts* are published online shortly after acceptance, before technical editing, formatting and proof reading. Using this free service, authors can make their results available to the community, in citable form, before we publish the edited article. We will replace this *Accepted Manuscript* with the edited and formatted *Advance Article* as soon as it is available.

You can find more information about *Accepted Manuscripts* in the [Information for Authors](#).

Please note that technical editing may introduce minor changes to the text and/or graphics, which may alter content. The journal's standard [Terms & Conditions](#) and the [Ethical guidelines](#) still apply. In no event shall the Royal Society of Chemistry be held responsible for any errors or omissions in this *Accepted Manuscript* or any consequences arising from the use of any information it contains.



Analyst

PAPER

## Depth resolution at organic interfaces sputtered by argon gas cluster ions: the effect of energy, angle and cluster size

M. P. Seah,<sup>a</sup> S. J. Spencer,<sup>b</sup> R. Havelund,<sup>b</sup> I. S. Gilmore<sup>b</sup> and A. G. Shard<sup>b</sup>

Received 00th January 20xx,  
Accepted 00th January 20xx

DOI: 10.1039/x0xx00000x

www.rsc.org/

An analysis is presented of the effect of experimental parameters such as energy, angle and cluster size on the depth resolution in depth profiling organic materials using Ar gas cluster ions. The first results are presented of the incident ion angle dependence of the depth resolution, obtained at the Irganox 1010 to silicon interface, from profiles by X-ray photoelectron spectrometry (XPS). By analysis of all relevant published depth profile data, it is shown that such data, from delta layers in secondary ion mass spectrometry (SIMS), correlate with the XPS data from interfaces if it is assumed that the monolayers of the Irganox 1010 adjacent to the wafer substrate surface have an enhanced sputtering rate. SIMS data confirm this enhancement. These results show that the traditional relation for the depth resolution,  $\text{FWHM} = 2.1 Y^{1/3}$ , is slightly better,  $\text{FWHM} = P_X Y^{1/3}/n^{0.2}$ , where  $n$  is the argon gas cluster size, and  $P_X$  is a parameter for each material are valid both at the 45° incidence angle of the argon gas cluster sputtering ions used in most studies and at all angles from 0° to 80°. This implies that, for optimal depth profile resolution, 0° or >75° incidence may be significantly better than the 45° traditionally used, especially for the low energy per atom settings required for the best resolved profiles in organic materials. A detailed analysis, however, shows that the FWHM requires a constant contribution added in quadrature to the above such that there are minimal improvements at 0° or greater than 75°. A critical test at 75° confirms the presence of this constant contribution.

### Introduction

The depth profiling of organic materials is important for the analysis of layered organic coatings, organic electronics and such studies as the location of drugs in biological materials studied by secondary ion mass spectrometry (SIMS). Achieving high-resolution depth profiles is critical to many applications. The depth resolutions in sputter depth profiling using Auger electron spectroscopy (AES), X-ray photoelectron spectroscopy (XPS) and SIMS have been of major importance since the earliest uses of the methods. In complex samples, the resolution could be dependent on the crystallinity of the layers sputtered<sup>1</sup> and this explained some of the poor resolutions observed early in AES studies.<sup>2</sup> However, for amorphous layers on well-defined substrates, excellent depth resolution has been achieved by many laboratories.<sup>3</sup> Low energies invariably improved results.<sup>2-7</sup> For many samples, changing the angle of incidence did not improve matters since the roughness of the substrate<sup>3</sup> dominated effects at high angles of incidence. However, for samples on polished Si wafers, the resolution generally improved as the angle of incidence increased.<sup>8</sup> Sometimes, if the

primary ion was incorporated in the sample, the resolution degraded around 45°. At very grazing incidence, using monatomic Ar<sup>+</sup> ions, extremely good depth resolutions could be achieved.<sup>10</sup> For inorganic or elemental samples using monatomic primary ions, there is thus an extensive knowledge base and generally very clear concepts on which the analyst can build to devise the most appropriate conditions for efficient and high-resolution depth profiling of samples. The situation for organic materials, which are sputtered today using argon gas cluster ion beams (Ar GCIBs), is not so clear since the theory is less well established and the experimental characterisation of effects is very limited. In the present work, we seek to establish part of this framework with new measurements as a function of incidence angle.

Currently, few angle dependent depth-resolution measurements exist for organic materials sputtered using argon gas cluster ions. Many depth profiles have been made in organics using SIMS but in these the experiments are mainly limited to one angle of incidence. In early work with C<sub>60</sub><sup>+</sup> at 45° incidence angle, Shard *et al.*<sup>11</sup> show, using organic delta layer samples, that reducing the energy was always beneficial to depth resolution although at low energies the deposition of carbon and the damage to the sample meant that the profile was then of poor quality or, sometimes, not at all meaningful. In that work, based on a simple model, it was shown that the full widths at half maximum (FWHM) of the delta layers at energies from 10 to 40 keV were, on average, equal to  $3Y^{1/3}$ , where  $Y$  was the sputtering yield expressed as a volume. For sputtering using Ar<sub>*n*</sub><sup>+</sup> the unwanted degradation effects of C<sub>60</sub><sup>+</sup> were removed

<sup>a</sup> Analytical Science Division, National Physical Laboratory, Teddington, Middlesex TW11 0LW, UK. E-mail: [martin.seah@npl.co.uk](mailto:martin.seah@npl.co.uk)

<sup>b</sup> Analytical Science Division, National Physical Laboratory, Teddington, Middlesex TW11 0LW, UK.

† Footnotes relating to the title and/or authors should appear here.

Electronic Supplementary Information (ESI) available: [details of any supplementary information available should be included here]. See DOI: 10.1039/x0xx00000x

and Shard *et al.*<sup>12</sup> show excellent results for 2.5 keV Ar<sub>1700</sub><sup>+</sup> primary ions. Data from four laboratories, all at 45° incidence angle, supported the relation FWHM = 3Y<sup>1/3</sup> for beam energies between 2.5 and 4 keV and cluster sizes from  $n = 1700$  to 2500. Niehuis *et al.*<sup>13</sup> have measured the depth resolutions, using the 16% to 84% criterion for the organic light emitting diode materials, NPB (4,4'-bis[N-(1-naphthyl-1-)-N-phenyl-amino]-biphenyl, C<sub>44</sub>H<sub>32</sub>N<sub>2</sub> with molecular mass 588.75 Da), HTM-1 (2,2',7,7'-tetra(N,N-ditolyl)amino-9,9-spiro-bifluorene, C<sub>81</sub>H<sub>68</sub>N<sub>4</sub> with molecular mass 1096.54 Da) and Irganox 1010 (C<sub>73</sub>H<sub>108</sub>O<sub>12</sub> and molecular mass 1176.78 Da) for a wide range of conditions with energies between 2.5 and 20 keV and cluster sizes from  $n = 500$  to  $n = 5000$ , all at 45° incidence angle. For NPB, there is a dramatic improvement in depth resolution at the higher energies as  $n$  increases. For HTM-1, a rough correlation is shown for the FWHM and  $r$  the radius of the crater hemisphere representing the sputtering yield volume  $Y$  (i.e.  $2/3\pi r^3 = Y$ ). On the plot for the 16% to 84% depth resolution,  $\Delta z$ , versus sputtering yield radius,  $r$ , the gradient  $\Delta z/r$  falls from  $\sim 2.4$  for  $n = 500$  to 2.2 for  $n = 2000$  and 1.9 for  $n = 5000$ . These are similar to Shard *et al.*'s<sup>12</sup> results but they also show an effect for  $n$ . Data are also provided for the depth resolution in Irganox 1010 which show a very small increase with sample depth, especially at the lower  $E/n$  values. This increase is removed using sample rotation.<sup>13</sup> At 5 keV beam energy and  $n = 5000$ , the depth resolutions were around 4 to 5 nm. These are the level of the best depth resolutions so far achieved for the argon gas cluster sputtering of organic materials in SIMS.

We know that the sputtering yield changes<sup>14,15</sup> with the argon gas cluster ion beam angle of incidence,  $\theta$ , but, as yet there are no data for the angular dependence of the depth resolution. Both the analogue with monatomic Ar sputtering of inorganic materials and the relation to  $Y^{1/3}$  indicate a possibly strong effect. In recent work, Seah *et al.*<sup>15</sup> show that the angle dependence of the sputtering yield of Irganox 1010 may be described by the following equations

$$A(\theta) = A(0^\circ) \left[ \frac{1 + F \exp(-\theta^2 / 2\theta_0^2)}{(1 + F) \cos(\theta)} \right] \quad (1)$$

where  $A(\theta) = 4.1$  eV,  $F = 3.1$  and  $\theta_0 = 18^\circ$ . In eqn (1),  $A(\theta)$  is the parameter given in the Universal Sputtering Equation describing the sputtering yield volume<sup>15-17</sup>

$$\frac{Y}{n} = \frac{B \{E / [A(\theta)n]\}^q}{(1 + \{E / [A(\theta)n]\}^{(q-1)})} \quad (2)$$

Here  $B$  is an experimentally determined parameter with the same units as  $Y$ . Equation (2) was evaluated for many systems but with most of the data for 45° incidence<sup>16</sup> except, more recently, for Irganox 1010 at many angles.<sup>15</sup> Here, for Irganox 1010,  $B = 0.0176$  nm<sup>3</sup> and the units of  $Y$  are taken as a volume. These relations, with different values for the parameters, also accurately describe the polystyrene data of Rading *et al.*<sup>14</sup> for the angle dependence of the argon gas cluster ion sputtering yield. Thus, as with the sputtering of elemental and inorganic materials, the yield changes slowly

around  $\theta = 0^\circ$ , rises to a peak around the middle angles and finally falls to zero at 90°. The behaviour is similar to monatomic sputtering but the physics of the process is quite different<sup>15</sup> and so it is not clear how the depth resolution should alter with  $\theta$ . In the present work, we measure the depth resolution for Irganox 1010 films deposited on Si wafers as a function of  $\theta$  for many  $E/n$  combinations in the useful working range using XPS to monitor the sample surface. Angle dependent measurement for layers is relatively straightforward in XPS instruments although the signal level for the delta layers that are often studied in SIMS is generally too poor.

As a result of certain issues that the XPS results raise, a detailed analysis is made of the SIMS depth profiles reported by Niehuis *et al.*<sup>13</sup> before reporting complementary data using SIMS. Unfortunately, in the instrument used and as in most SIMS instruments, all the argon cluster ion sputtering is designed to be made at 45° incidence to the surface normal or the whole experiment could have been conducted by SIMS. However, the use of these two instruments provides a very interesting combined result.

## Experimental

The experimental arrangement for the XPS measurements was the same here as described by Seah *et al.*<sup>15</sup> Briefly, depth profile measurements were conducted in a Axis Ultra DLD X-ray photoelectron spectrometer (Kratos, UK) to which a GCIB 10S argon cluster ion gun (Ionoptika, UK) had been added at 65° to the spectrometer input lens axis. The gun is set to select a narrow band of cluster sizes. The X-ray monochromator is set at 60° to the input lens axis in the azimuth opposite to that of the ion gun. The ion beam incidence angle was set by tilting the sample on an axis that is normal to the azimuths containing the X-ray monochromator and the ion gun.

For the XPS data, samples of 10 mm squares of silicon wafer, with single layers of approximately 50 nm of Irganox 1010, were prepared with thicknesses measured using an M-2000D spectroscopic ellipsometer (Woollam, US). Profiling of most of the samples was conducted by repeated cycles of sputtering  $\sim 1$  nm of Irganox 1010 at the required angle of incidence of the argon beam, following which the sample was reset with its normal along the spectrometer input lens axis and the XPS measurement made. Those at 45°, 60° and 70° could be profiled without resetting the sample.

The XPS source was of monochromated Al K $\alpha$  X-rays that illuminate approximately an area 1 mm by 2 mm on the sample but the analyser was set to analyse a region of only  $\sim 220$   $\mu$ m diameter to obtain good depth resolution. The carbon 1s and silicon 2p XPS regions were measured using the instrument in the snapshot mode where  $\sim 0.1$  eV steps for  $\sim 14.5$  eV of the binding energy scale are recorded simultaneously. The charge neutraliser and X-ray source were only used during the acquisition of spectra, both being turned off during the sputtering cycle. The ion beam was rastered to sputter a region on the sample of sides 1.4 mm to 2.6 mm by 3.6

mm for angles of incidence up to 60°, above which the rastered region became an elongated rectangle up to 6.4 mm by 3.6 mm. The sputtered areas were measured optically from each crater.

The SIMS depth profiles were conducted using a TOF-SIMS IV (ION-TOF, Germany) equipped with an argon cluster ion source for sputtering and a 25 keV Bi<sub>3</sub><sup>+</sup> liquid metal ion source for analysis. The argon cluster ion source uses a 90° pulsing system to provide a mass-selected ion pulse ( $n/\Delta n$  between 60 and 120). In this study, argon cluster sizes ranging from  $n = 500$  to  $n = 7500$  and energies between 2.5 and 20 keV were used, incident at 45° to the surface normal. The dc ion beam current was measured in a Faraday cup on the sample holder for each beam condition. The Bi<sub>3</sub><sup>+</sup> beam was also at 45° to the surface normal but in an azimuth at 90° to that of the argon gas cluster beam. The Bi<sub>3</sub><sup>+</sup> beam currents were typically ~0.10 pA at 5 kHz pulse rate, analysing an area of 200 μm × 200 μm in the centre of a 450 μm × 450 μm argon sputter crater. Analysis was conducted in the interlaced mode and charge compensation was used.<sup>29</sup>

For the SIMS data, samples of 10 mm squares of silicon wafer, with 1 nm Irganox 3114 layers at nominal depths of 50, 100, 200 and 300 nm of Irganox 1010 over a further 100 nm layer of Irganox 1010 were prepared, as described earlier,<sup>12</sup> with precise thicknesses measured, as above, by spectroscopic ellipsometry. All SIMS studies were conducted at 45° incidence angle as required by the instrument design except the final measurement for which a specially designed electrode arrangement allowed an edge of the sample to be analysed at 75° incidence whilst maintaining the ion extraction field in its normal configuration. To avoid excessive Bi<sub>3</sub><sup>+</sup> analysis beam damage with the very low sputtering rate for the argon cluster beam at this angle of incidence, the mode was changed to non-interlaced.

Atomic force microscopy of both the wafer substrates and the finished materials<sup>11</sup> showed roughnesses below 1 nm.

## Results and discussion

**A. XPS data for the Irganox 1010 on Si sample.** In this study, we have measured the depth resolution at the interface by measuring the C 1s intensity, characterising the Irganox 1010, as a function of the sputtering dose. The dose rate is calculated directly from the argon gas cluster beam current and the measured raster area for each profile. The XPS intensity is determined from the peak area in the snapshot mode energy spectrum above a straight line background. An example widescan spectrum is shown in Fig. 1 of Seah *et al.*<sup>15</sup> and the snapshot mode spectra are very similar to those given by Figs. 5(a), (c) and (d) of the earlier study<sup>17</sup> using coronene primary ions showing no Irganox 1010 damage by the Ar GCIB.

A typical depth profile for 10 keV Ar<sub>5000</sub><sup>+</sup> is shown in Fig. 1 for both the C 1s and Si 2p peak areas as a function of the argon cluster ion dose. The method of repeated cycles means that the data points are generally separated by 0.5 to 1 nm of Irganox 1010 removal. The spacing of the data points means that the detail at the interface

is poor and the method used previously for the delta functions in Irganox 1010 measured with SIMS<sup>12,17</sup> is not possible. There, Dowsett's asymmetric resolution function<sup>7,18</sup> was used and was found by Shard *et al.*<sup>11,12</sup> to describe both the measured profile shape for delta layers as well as the roughness histogram for the sputtered Irganox 1010 surface measured by atomic force microscopy. This asymmetric function includes three parameters: an exponential growth parameter, a Gaussian roughness parameter and an exponential decay parameter; the overall functions being a convolution of the three terms. Instead of this 3-parameter function, we shall use a simple Gaussian profile as this requires fewer data points for fitting. The fitted integral Gaussian is shown for the C 1s data in Fig. 1. In addition, the C 1s intensity shows a slow decline through the data. This was thought to arise from the X-ray monochromator source intensity falling during the profile – sometimes the intensity rose slightly. It is not thought that the issues of heating and degradation seen by Cumpson *et al.*<sup>19</sup> are significant here since the X-ray monochromator covers an area 200 times larger (and therefore this amount lower in flux density) than compared with Cumpson *et al.*'s study and has concomitantly lower X-ray doses.

The measured full widths at half maximum (FWHM) intercalculated from  $2[2\ln(2)]^{0.5}$  times the standard deviation in the Gaussian fitted function, are for  $0^\circ \leq \theta < 80^\circ$ , with  $E = 5$  keV and 10 keV and  $n = 1000, 2000, 4000$  and 5000. These FWHMs, in terms of dose, are simply converted to a FWHM in nm by multiplying by the measured film thickness divided by the dose to the interface. Analysis using the Si 2p peak instead of C 1s gives similar FWHM values with a root mean square difference of 0.65 nm. The results for the 6 combinations of  $E$  and  $n$  are shown in Fig. 2 where it is clear that good resolutions are seen at both high and low angles of incidence whereas at 45° the resolutions are generally poorest. It is also clear that the best resolutions occur at the lowest  $E/n$  values and vice versa. These conclusions echo the effect of the angle of incidence on the sputtering yields,  $Y$ , reported by Seah *et al.*<sup>15</sup> for various  $E$  and  $n$  combinations and so we consider how the dependence of FWHM on  $Y$  noted in the Introduction changes with  $\theta$ . Figure 3 shows the plot of FWHM versus  $Y^{1/3}$  with the data for each angle separately colour coded. There is a significant scatter. Within this scatter, there is no obvious dependence on  $\theta$ . There is clearly an issue here since the depth resolution, at best, is ~1.4 nm and we know that, if the interface is really of zero thickness, the C 1s signal,  $I$ , should follow the function<sup>20,21</sup>

$$I = I_0 \{1 - \exp[-x/(L \cos \alpha)]\} \quad (3)$$

where  $I_0$  is the intensity significantly before the interface,  $x$  is the distance to the interface,  $L$  is the attenuation length of the C 1s electrons and  $\alpha$  the angle of emission of these electrons from the surface normal. Using Al K $\alpha$  X-rays, the attenuation length for the C 1s electrons,  $L$  is 3.3 nm.<sup>20,21</sup> If we fit a Gaussian to the simple function of eqn (3), the fit would be poor and its FWHM would be ~5.5 nm, i.e. the minimum resolution, which is for an ideally sharp interface, is 5.5 nm. Thus, there is clearly a compression of the depth scale at the interface of the profiles. Figures 4(a) and (b) show details of the interfaces for 5 keV Ar<sub>1000</sub><sup>+</sup> sputtering at 0° and

80° incidence angles, respectively. The curves for eqn (3), for the relevant values of  $\alpha$ , are shown each time in red, set to terminate at the centroids of the fitted Gaussians. The measured interfaces are too sharp and do not follow the predicted shape. What these curves appear to show is that around the interface, the final 2 to 3 nm or so of material simply disappears, perhaps with a high sputtering yield. Thus, the resolution from interfaces of dissimilar materials may be biased but may still give the correct trends.

The Irganox 1010 molecule is of a tetragonal shape with 4 symmetrical arms that interlock with each other in the solid state but which do not bond especially to the hydrated SiO<sub>2</sub> layer on the Si substrate.<sup>22</sup> We may therefore expect the final layer(s) of Irganox 1010 to be weakly adsorbed and sputtered with a significantly higher yield than the rest of the material. Additionally, the higher density and low sputtering yield of the substrate may localise the deposited ion energy so enhancing the sputtering yield of these final layers. Thus, the final layer of ~1 to 2 nm (the molecular volume is 1.7 nm<sup>3</sup>) is rapidly removed. The apparent thickness that is lost may be greater than this and may depend on either  $Y$  or  $\theta$ .

To try to evaluate this missing information, it is worth re-visiting the depth resolution data cited in the Introduction for SIMS measurements on delta layers,<sup>13</sup> rather than at an Si interface, since that removes the issue of the change in sputtering yield of the Irganox 1010 near the Si interface but, unfortunately, the data are all at 45°. Figure 5(a) shows the depth resolution data from Niehuis *et al.*<sup>13</sup> for a 20 nm layer of NPB on a 60 nm layer of HTM-1 that is, in turn, on an indium tin oxide substrate as well as data for the delta layers in an NPL Irganox 1010 reference sample described in the Experimental section. In their publication, Niehuis *et al.*<sup>13</sup> provide a depth resolution,  $\Delta z$ , from the 16% to 84% criterion for layer interfaces from which we may derive the FWHM as  $[2\ln(2)]^{0.5}$  times that value. The NPB and HTM-1 data are from the falling and rising intensities, respectively, at the first interface at 20 nm depth, whereas the Irganox data are those for the first delta layer at 50 nm depth. The yields for the abscissa are calculated from the Universal Equation of eqn (2) for HTM-1 and Irganox 1010 using the parameters given by Seah<sup>16</sup> and for NPB given by Holzweber *et al.*<sup>23</sup> It is not clear if the HTM-1 result should use the yield for the overlayer (NPB) or that for the material giving the signal (HTM-1). Niehuis *et al.*<sup>13</sup> use the latter and we shall follow that procedure, noting that in this case the similarities in the yield make these numerically the same. The correlation here in Fig. 5(a) gives, for the three organic materials:

$$\text{FWHM} = 2.1Y^{1/3} \quad (4)$$

The scatter of the points about the line is 1.8 nm. Niehuis *et al.*<sup>13</sup> derive the radius  $r$  of a typical crater as a hemisphere of volume  $Y$  so that  $Y^{1/3} = (2\pi/3)^{1/3}r$ , giving  $\Delta z = 2.3r$ , as shown in their Fig. 4. In Fig. 5, Niehuis *et al.*'s<sup>13</sup> Fig. 4 and other data are reworked to investigate the resolution dependence on  $Y$  and  $n$  more fully. Here, the round symbols are for NPB, the triangles for HTM-1 and the squares for Irganox. The associated numbers in the key are the cluster sizes. In Fig. 5(a), it is clear that low cluster sizes are

generally above the line and high ones below the line, indicating a dependence on  $n$ . Including  $n$  into the fit we get

$$\text{FWHM} = P_x \frac{Y^{1/3}}{n^{0.2}} \quad (5)$$

where  $P_x = 10.5$  for NPB, 9 for HTM-1 and 8.5 for Irganox 1010. Since we may expect that the depth resolutions may be material and sample-fabrication dependent. This result, using the data shown in Fig. 5(a), is shown in Fig. 5(b) with the FWHM as ordinate and the right hand side of eq (5) as abscissa. The scatter is now reduced to 1.0 nm. However, it is also likely that, for the same  $n$  value, increases in  $E$  lead to a crater whose aspect ratio deepens rather than being fixed, i.e the true power for  $Y$  may be slightly greater than 1/3.

Observing Fig. 5(b), it is clear that the data at low abscissa values may not extrapolate to zero but the line may be curved and the data could be fitted to a function including a constant contribution. Fitting such a function to those data leads to

$$\text{FWHM} = \left[ (\text{FWHM}_0)^2 + \left( R_x \frac{Y^{0.6}}{n^{0.3}} \right)^2 \right]^{0.5} \quad (6)$$

where  $\text{FWHM}_0 = 4.75$  nm and  $R_x = 6$  nm<sup>-0.8</sup> for NPB, 5 nm<sup>-0.8</sup> for HTM-1 and 4 nm<sup>-0.8</sup> for Irganox 1010. This result is shown in Fig. 5(c), with the FWHM as ordinate and the right hand side of eqn (6) as abscissa. The scatter is now reduced further to 0.7 nm. The difference between the linear results of Figs. 5(a) and (b) and the result of Fig. 5(c) is very important for those considering improving the depth resolution. The linear plots indicate a significant improvement if the yield is reduced further whereas the latter indicates little effect. Contributions to  $\text{FWHM}_0$  are expected from the intrinsic width of any delta layer, the evenness with which organic layers may be deposited, the characteristic analysis depth for the analysis ion, the morphology and any mixing developed by the Ar gas cluster sputtering beam.

Note that, in terms of  $r$ , the FWHM of eqn (4) is  $2.7r$ . The FWHM for the first layer sputtered may be close to  $r$  but an increase to  $2.7r$  is the level of increase, at equilibrium, compared with the first layer, that is calculated by Seah *et al.*<sup>24</sup> This is the increase for the sequential layer sputtering model when elevated parts (e.g. a prior crater rim) are sputtered more easily than re-entrant parts (e.g. a prior crater floor).

We now consider the XPS data measured here and presented earlier in Figs. 2 and 3. We may use either eqn (4), (5) or (6) to calculate the FWHM that would be observed in SIMS for delta layers, convolve that with the effect of eqn (3) and compare that with the value measured here at the interface by XPS at each of the angles of incidence,  $\theta$ . Equations (4) and (5) imply no intrinsic effect of the SIMS analysis but in eqn (6) it may be that the  $\text{FWHM}_0$  value, or part of that value, is associated with the SIMS itself and should be removed in whole or in part. Figure 6(a) shows this with eqn (5) for Irganox 1010 used for the abscissa. The result using eqn (4) is

similar but a little more scattered. The dashed curve is the ideal correlation that includes the attenuation length for the photoelectrons. It is clear that all of the data points lie below this curve as a result of the rapid removal of the final monolayers. It is straightforward to calculate the profile including the attenuation length, then to remove a thickness of material and fit an integral Gaussian to the result. For each data point we may, in this way determine the apparent layer thickness,  $z_0$ , so removed. This thickness shows no significant dependence on  $E/n$  or  $\theta$  and averages 3.5 nm with a standard deviation of the mean of 0.15 nm. The solid curve shows the fit with the removal of the average 3.5 nm layer. The data scatter about this line with a standard deviation of 1.0 nm. Figure 6(b) shows the average value of  $z_0$  for each value of  $\theta$ . There is clearly no significant trend with  $\theta$ . This is not obvious since one may expect the shapes of craters to alter with  $\theta$  so that the depth resolution for a given  $Y$  changes with  $\theta$ . However, the molecular dynamics calculations of Czerwinski *et al.*<sup>25</sup> show clearly craters of the same depth for 14.75 keV Ar<sub>366</sub><sup>+</sup> at 0° and 45° where the sputtering yields are the same. The craters have slightly different shapes but the same depth.

It appears, therefore, as though some 3 to 4 nm, for the final layer in contact with the substrate, has a high yield and is effectively lost to this depth resolution measurement. This is not easy to prove since evidence of something missing is far harder to establish than that for something observed. However, we can be sure that the XPS depth resolution should be poorer (because of the added attenuation length contribution) than that observed had the sputtering rate been uniform.

We have, in the past, noted that the sputtering rate of materials at the surface will generally be higher than at equilibrium<sup>26</sup> and the rate at the interface may be either higher or lower depending on the bonding to the substrate and, for monatomic ions, the stopping power of the substrate. The linearity of the sputtering rate within the bulk of the Irganox 1010 may be confirmed in the SIMS depth profiling of the delta-layer materials mentioned above.

**B. SIMS data for the delta-layer sample.** Figure 7(a) shows an example depth profile using the (M-H)<sup>-</sup> secondary ion to characterise the Irganox 1010 matrix and the intense (CNO)<sup>-</sup> ion, the Irganox 3114 delta layers. Measurements for four strong Irganox 3114 secondary ions show very similar profiles except that they are each shifted slightly with respect to each other on the dose scale. Such profiles are not possible by XPS since the delta layer intensities are then too weak for good measurements. Figure 7(a) is actually measured as a function of dose rather than depth and the conversion is made as shown in Fig. 7(b) using the measured layer thicknesses. For Fig. 7(b), we have fitted the depth profile data for each delta layer separately using Dowsett's function<sup>7,8</sup> as shown by the black line in Fig. 7(a), and then evaluated the centroid of each peak on the intensity-dose plot. That dose defines the centre of each 1.0 nm Irganox 3114 layer whose centroid depths in nm then provide the ordinate scale in Fig. 7(a). The gradient of the line in Fig. 7(b) between the four delta layers (red points) gives the steady state sputtering yield which, here, for 5 keV Ar<sub>2000</sub><sup>+</sup>, is 37.59 nm<sup>3</sup> with a standard deviation of only 0.02 nm<sup>3</sup> for the four secondary

ions: CN<sup>-</sup>, CNO<sup>-</sup>, C<sub>18</sub>H<sub>24</sub>N<sub>3</sub>O<sub>4</sub><sup>-</sup> and C<sub>33</sub>H<sub>46</sub>N<sub>3</sub>O<sub>5</sub><sup>-</sup>. The straight line in Fig. 7(b) is extended beyond the four delta layer points to the green square at zero and the blue square at the Irganox 1010 to Si interface. To pass through these points, the extensions would need to be slightly non-linear. The non-linear result at the Si interface is particularly important as this may tell if any material is rapidly removed. To address this we first need to consider the reasons for non-linear results with depth. Firstly, near zero depth before any damage or ion inclusion occurs, the sputtering rate for the first monolayers will probably be higher than for the rest of the bulk, as usually observed. Secondly, the 25 keV Bi<sub>3</sub><sup>+</sup> analysis ion ejects material from depths of up to 2 nm below the surface so seeing layers just before the interface is reached and thirdly, matrix effects cause the intensities not to be linearly related to quantity and this causes apparent shifts. Thus the centroids for CN<sup>-</sup> and CNO<sup>-</sup> appear at 0.65 ± 0.04 nm and 1.20 ± 0.06 nm before the average of all four secondary ions and C<sub>18</sub>H<sub>24</sub>N<sub>3</sub>O<sub>4</sub><sup>-</sup> and C<sub>33</sub>H<sub>46</sub>N<sub>3</sub>O<sub>5</sub><sup>-</sup> appear at 1.56 ± 0.06 nm and 0.30 ± 0.03 nm afterwards.

At the fourth delta layer, the profiles are shown in Fig. 7(c). The profile depth is calculated from the dose using the average sputtering yield (37.59 nm<sup>3</sup>) and offset (1.63 nm). The true position of the delta layer is indicated by the dashed rectangular profile from 300.2 to 301.2 nm depth. We can see the above shifts clearly. They are repeatable. Also shown is the Irganox 1010 (M-H)<sup>-</sup> ion (line C<sub>73</sub>H<sub>107</sub>O<sub>12</sub><sup>-</sup>). The minimum for this ion at the delta layer has a centroid at 301.2 nm, some 0.5 nm deeper than the average for the four Irganox 3114 ions. This is about where one would expect the larger ion to appear but it is clear that the measurement of such a minimum may have an error of up to 0.5 nm. The minimum in intensity is equivalent to a layer of Irganox 3114 that is 0.98 nm thick, confirming the data quality and is indicative of minimal matrix effects.<sup>27</sup>

At the interface, the results are shown in Fig. 7(d). The intensities for the Irganox 1010 fragments exhibit a fairly flat response ending in an integral Gaussian decay. In Fig. 7(d) the intensity for the C<sub>2</sub>H<sub>2</sub>O<sub>2</sub><sup>-</sup> and C<sub>16</sub>H<sub>23</sub>O<sup>-</sup> secondary ion fragments are separately fitted with interfaces at 396.6 nm (where the 50% intensity point occurs), 3.8 nm short of the expected 400.4 nm. The results for C<sub>2</sub>H<sub>3</sub>O<sub>2</sub><sup>-</sup> and C<sub>17</sub>H<sub>25</sub>O<sub>3</sub><sup>-</sup>, not shown, are very similar with their interfaces within 0.4 nm of the 396.6 nm value. These results are consistent with an enhanced sputtering rate equivalent to 3.8 nm of material next to the Si interface, and in agreement with the difference of 3.5 nm between the solid line and the dashed line for the XPS data in Fig. 6(a).

The results of Fig. 6(a), and the traditional approach leading to Figs. 5(a) and (b), indicate an improved resolution for SIMS at low  $Y$  values whereas Fig. 5(c) indicates no significant improvement. It is very important to confirm which of these approaches is correct for future developments and so SIMS data were recorded using 75° incidence for 5 keV Ar<sub>2000</sub><sup>+</sup> ions for the Irganox 3114 in Irganox 1010 delta layer sample. A sample was mounted on a 30° wedge to do this. A razor blade was mounted horizontally (the correct sample orientation) over the multilayer sample, exposing only a small area near the razor edge. This was done to overcome the extraction field

trajectory distortion.<sup>28</sup> The razor edge was necessary to avoid the sputtering of material from this field-maintaining electrode onto the area being profiled. Under these conditions, the sputtering yield is reduced to a measured 2.5 nm<sup>3</sup> compared with 40 nm<sup>3</sup> at 45° incidence. This is consistent with eqns (1) and (2). The measured FWHMs for the first delta layer for m/z = 26 and 564 are 6.6 and 6.4 nm, respectively. In terms of the plots for Figs. 5(b) and (c), this result is at half the abscissa value for the lowest plotted point where the predictions for eqs (5) and (6) are 2.5 nm and 5 nm, respectively. This is where any discrepancy is best observed. The measured result confirms the results of Fig. 5(c) and eq (6), showing that we cannot expect the resolution to improve significantly for conditions with sputtering yields below 40 nm<sup>3</sup>.

## Conclusions

Depth profiles of Irganox 1010 on Si using both XPS and SIMS show that the sputtering rate of the final 3 to 4 nm at the Si surface is elevated. This is thought to arise from the low binding energy of the molecules to the hydrated oxide on the silicon surface and, or, the higher energy deposition density at the organic/inorganic interface. This leads to profiles in XPS that appear sharper at the interface than expected. If this offset is included, it is found that the FWHM in depth profiling is related to  $Y^{1/3}$  as given in eqn (4) with some scatter and that that scatter is reduced by including  $n$ , the number of atoms in the argon cluster, to generate eqn (5). A better equation, incorporating an intrinsic SIMS contribution and different powers for  $Y$  and  $n$  is given by eqn (6). These equations relate to NPB, HTM-1 and Irganox 1010 sputtered at 45° incidence angle. They are likely to be appropriate for all organic materials. These equations also appear to be valid for other angles up to 80°. If the offsets for the elevated interfacial sputtering yield are included, the equations for the 8 angles give the same coefficients as shown in eqs (4) and (5) to standard deviations of 6% and 5%, respectively, with no significant change with angle. Since, for any given  $E, n$  combination,  $Y$  is maximum close to 45°,<sup>15</sup> then a conclusion from the traditional approaches of eqs (4) and (5) would be that 45° would also give the poorest depth resolution for that  $E, n$  combination. The depth resolution at 0° and 75°, where for low  $E$  and high  $n$  combinations,<sup>15</sup>  $Y$  may be reduced 10 fold, the depth resolution would then be more than halved. Measurements at 75° show that this is incorrect and that the intrinsic component indicated in eqn (6) is essential and, leads to no significant improvement. Research needs to be focused on the contributions to this term to reduce it. Grazing incidence does not improve the depth resolution for Ar GCIBs in the manner commonly accepted for monatomic Ar when profiling inorganic materials. It is recommended that eqn (6) be used to evaluate or predict depth resolutions in SIMS and that a similar equation, with a different intrinsic component to allow for the electron escape depth, be used for XPS.

## Acknowledgements

The authors would like to thank Steve Smith for the preparation of samples, Ionoptika for assistance in the use of

the GCIB 10S, and the referees for helpful comments. This work forms part of the 3D NanoSIMS project in the Chemical and Biological programme of the National Measurement System of the UK Department of Business, Innovation and Skills and with funding by the European Metrology Research Programme (EMRP) projects NEW01-TREND and IND1-SurfChem. The EMRP is jointly funded by the EMRP participating countries within EURAMET and the European Union.

## References

- W. Höslér and W. Pamler, *Surf. Interface Anal.* 1993, **20**, 603-620.
- M. P. Seah and C. P. Hunt, *Surf. Interface Anal.* 1983, **5**, 33-37.
- C. P. Hunt and M. P. Seah, *Surf. Interface Anal.* 1983, **5**, 199-209.
- S. Hofmann, in *Practical Surface Analysis 2<sup>nd</sup> Edn. Vol 1 – Auger and X-ray Photoelectron Spectroscopy*, Eds. D. Briggs and M. P. Seah, Wiley, Chichester, 1990, Chapter 4 Depth Profiling in AES and XPS, 143-199.
- K. Wittmaack, in *Practical Surface Analysis, 2<sup>nd</sup> Edn Vol 2 – Ion and Neutral Spectroscopy*, Eds D. Briggs and M. P. Seah, Wiley, Chichester, 1992, Chapter 3 Basic Aspects of Sputter Depth Profiling, 105-175.
- M. G. Dowsett and E. A. Clark, in *Practical Surface Analysis, 2<sup>nd</sup> Edn Vol 2 – Ion and Neutral Spectroscopy*, Eds D. Briggs and M. P. Seah, Wiley, Chichester, 1992, Chapter 5 Dynamic SIMS and its Applications in Microelectronics in Practical Surface Analysis, 229-301.
- M. G. Dowsett, G. Rowlands, P. N. Allen and R. D. Barlow, *Surf. Interface Anal.* 1994, **21**, 310-315.
- M. G. Dowsett and R. D. Barlow, *Analytic Chimica Acta*, 1995, **297**, 253-275.
- M. Meuris, W. Vandervorst and J. Jackman, *J. Vac. Sci Technol. A*, 1991, **9**, 1482-1488.
- A. Barna, M. Menyhard, G. Zsolt, G. A. Koos, A. Zalar and S. Panjan, *J. Vac. Sci Technol. A* 2002, **21**, 553-557.
- A. G. Shard, F. M. Green, P. J. Brewer, M. P. Seah and I. S. Gilmore, *J. Phys. Chem. B* 2008, **112**, 2596-2605.
- A. G. Shard, R. Havelund, M. P. Seah, S. J. Spencer, I. S. Gilmore, N. Winograd, D. Mao, T. Miyayama, E. Niehuis, D. Rading and R. Moellers, *Anal. Chem.* 2012, **84**, 7865-7873.
- E. Niehuis, R. Möllers, D. Rading, H-G. Cramer and R. Kersting, *Surf. Interface Anal.* 2013, **45**, 158-162.
- D. Rading, R. Moellers, H-G. Cramer and E. Niehuis, *Surf. Interface Anal.* 2012, **45**, 171-174.
- M. P. Seah, S. J. Spencer and A. G. Shard, *J. Phys. Chem. B* 2015, **119**, 3297-3303.
- M. P. Seah, *J. Phys. Chem. C* 2013, **117**, 12622-12632.
- M. P. Seah, S. J. Spencer and A. G. Shard, *J. Phys. Chem. B* 2015, **117**, 11885-11892.
- M. G. Dowsett, J. H. Kelly, G. Rowlands, T. J. Ormsby, R. Guzman, P. Augustus and R. Beanland, *Appl. Surf. Sci.* 2007, **203-204**, 273-276.
- P. J. Cumpson, J. F. Portoles, N. Sano and A. J. Barlow, *J. Vac. Sci Technol. B*, 2013, **31**, 021208 1-11.

## Journal Name

- 1  
2  
3 20 M. P. Seah and S. J. Spencer, *Surf. Interface Anal.* 2011, **43**, 744-  
4 751.  
5 21 M. P. Seah, *Surf. Interface Anal.* 2012, **44**, 1353-1359.  
6 22 F. M. Green, A. G. Shard, I. S. Gilmore and M. P. Seah, *Anal.*  
7 *Chem.* 2009, **81**, 75-79.  
8 23 M. Holzweber, A. G. Shard, A. Jungnickel, A. Luch and W. E. S.  
9 Unger, *Surf. Interface Anal.* 2014, **46**, 936-939.  
10 24 M. P. Seah, J. M. Sanz, and S. Hofmann, *Thin Solid Films*, 1981,  
11 **81**, 239-246.  
12 25 B. Czerwinski, L. Rzeznik, R. Paruch, B. J. Garrison and Z.  
13 Postawa, *Nucl. Instrum. Methods B.* 2011, **269**, 1578-1581.  
14 26 M. P. Seah, C. P. A. Mulcahy and S. Biswas, *J. Vac. Sci Technol, B*  
15 2010, **28**, 1215-1221.  
16 27 A. G. Shard, S. J. Spencer, S. A. Smith, R. Havelund and I. S.  
17 Gilmore, I. S. *Int. J. Mass Spectrom* 2015, **377**, 599-609.  
18 28 J. L. S. Lee, I. S. Gilmore, M. P. Seah and I. W. Fletcher, *J. Am.*  
19 *Soc. Mass Spectrom.* 2011, **22**, 1718-1728.  
20 29 R. Havelund, M. P. Seah, A. G. Shard and I. S. Gilmore, *J. Am.*  
21 *Soc. Mass Spectrom.* 2014, **25**, 1565-1571.  
22  
23  
24  
25  
26  
27  
28  
29  
30  
31  
32  
33  
34  
35  
36  
37  
38  
39  
40  
41  
42  
43  
44  
45  
46  
47  
48  
49  
50  
51  
52  
53  
54  
55  
56  
57  
58  
59  
60

Analyst Accepted Manuscript

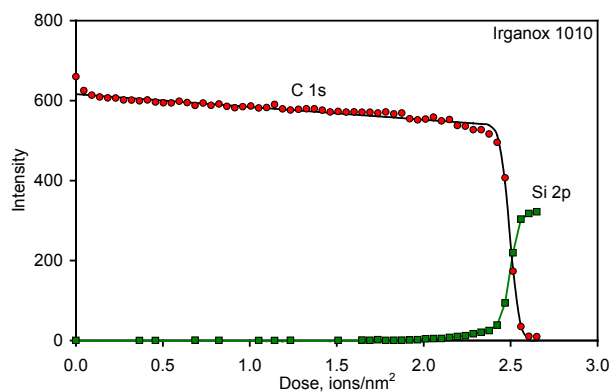


**Fig. 1** Depth profile showing the C 1s and Si 2p XPS intensities as a function of Ar gas cluster sputtering dose for a 49 nm thick Irganox 1010 layer sputtered with 10 keV  $\text{Ar}_{5000}^+$  ions incident at  $15^\circ$  from the surface normal.<sup>15</sup>

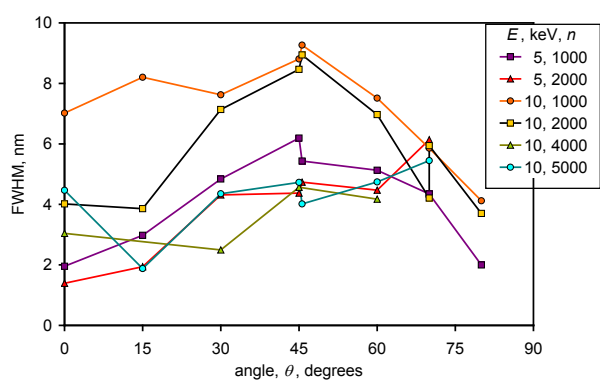


**Fig. 2** The measured FWHMs from the C 1s XPS peak as a function of the Ar gas cluster sputtering angle of incidence for the six  $E$  and  $n$  combinations for Irganox 1010. Analysis using the Si 2p peak instead of the C 1s peak gives similar FWHM values within a root mean square difference of 0.65 nm.

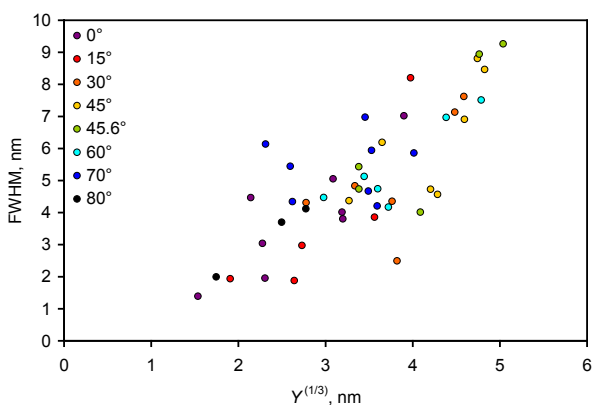


**Fig. 3** Measured FWHM from the XPS data for 5 and 10 keV  $\text{Ar}_n^+$  sputtering with  $n = 1000, 2000, 4000$  and 5000 at the Irganox 1010 to Si interface as a function of the cube root of the measured sputtering yield,<sup>15</sup>  $Y$ , for  $0^\circ \leq \theta \leq 80^\circ$ .

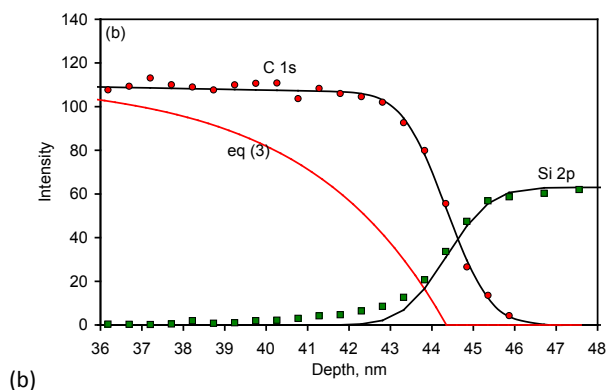
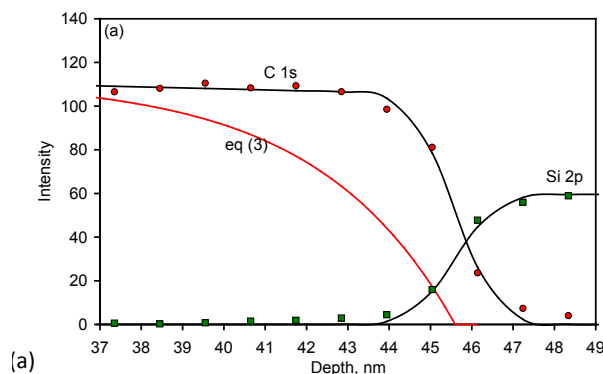


**Fig. 4** XPS profiles at the interface for 5 keV  $\text{Ar}_{1000}^+$  at (a)  $\theta = 0^\circ$  and (b)  $\theta = 80^\circ$ . The solid black lines are the integral Gaussian fits to the C 1s and Si 2p data with the Si 2p set to have the same mean position and FWHM as the C 1s data. The red curves represent eqn (3) with the interfaces set at the centroids for the C 1s profiles for illustrative purposes. Note that these two films have slightly different thicknesses.

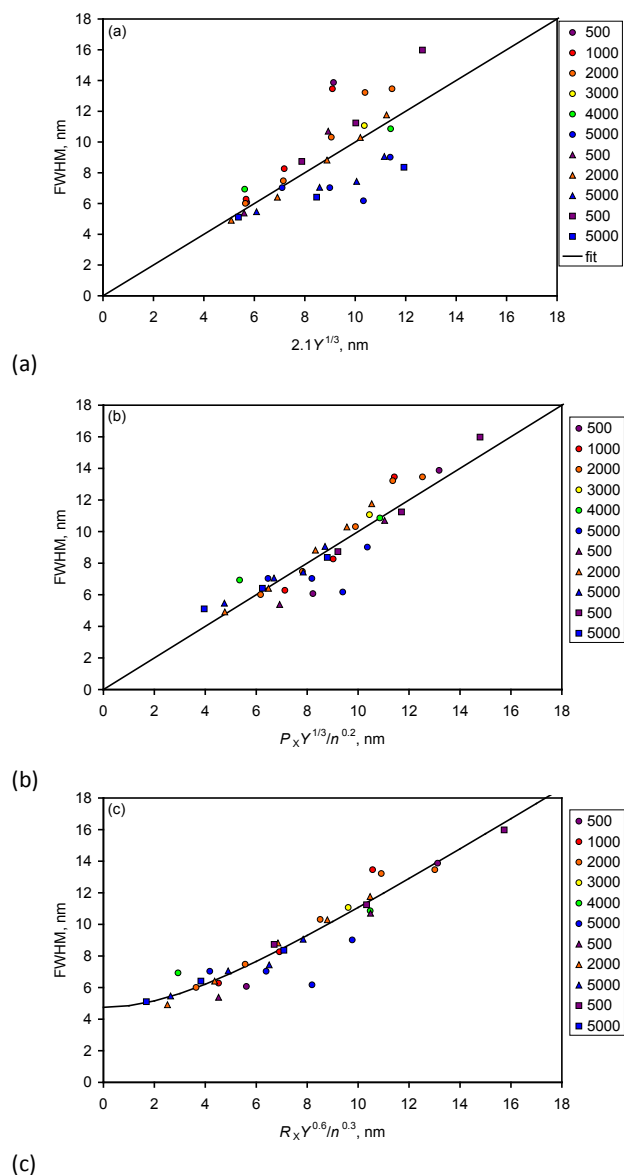


**Fig. 5** FWHMs for NPB (circles), HTM-1 (triangles), and Irganox 1010 (squares), using argon gas cluster ions, deduced from the depth resolutions in the SIMS depth profiles of Niehuis *et al.*<sup>13</sup> versus (a)  $2.1 Y^{1/3}$ , (b)  $P_x Y^{1/3} / n^{0.2}$  and (c)  $R_x Y^{0.6} / n^{0.3}$  where  $Y$  has been calculated from the Universal Equation. The numbers by the symbols give the cluster sizes. The energies range from 2.5 to 20 keV.

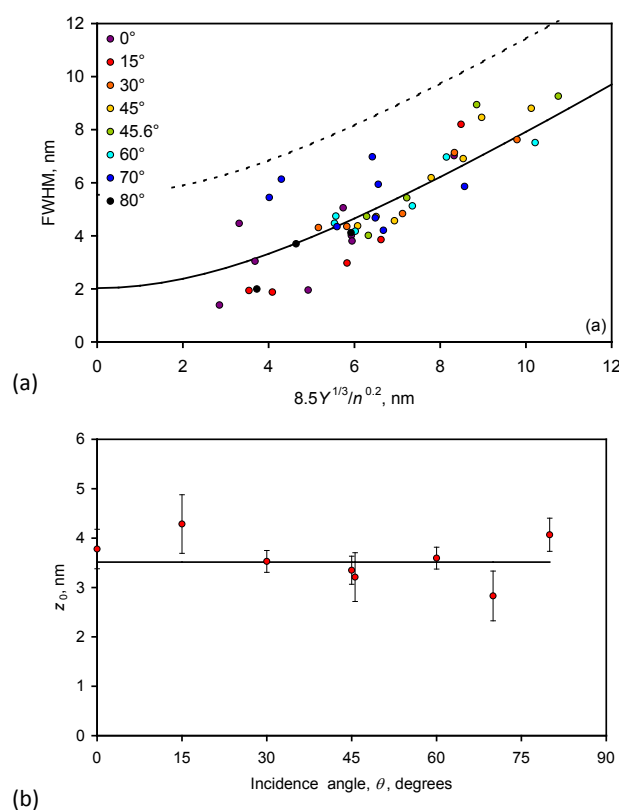


**Fig. 6** (a) Interface FWHMs for  $0^\circ \leq \theta \leq 80^\circ$  from the XPS depth profiles of Irganox 1010 on Si using argon gas cluster ions versus  $8.5 Y^{1/3} / n^{0.2}$  where  $Y$  has been determined from the Universal Equation by Seah *et al.*<sup>15</sup> The dashed line shows the calculated result allowing for the electron attenuation length and the solid line shows the expected result for 3.1 nm of rapidly sputtered material. (b) The mean thicknesses,  $z_0$ , of rapidly sputtered material for each  $\theta$ , plotted versus  $\theta$  with error bars showing the standard deviations of the means.

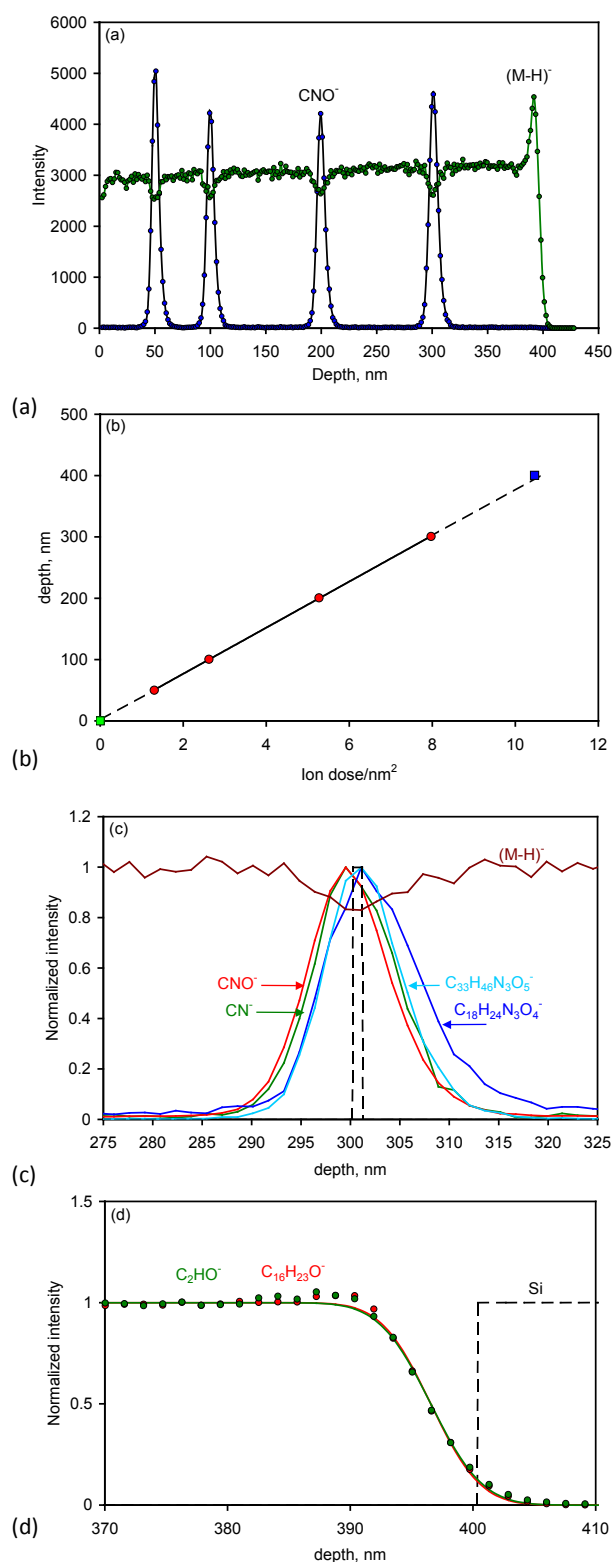
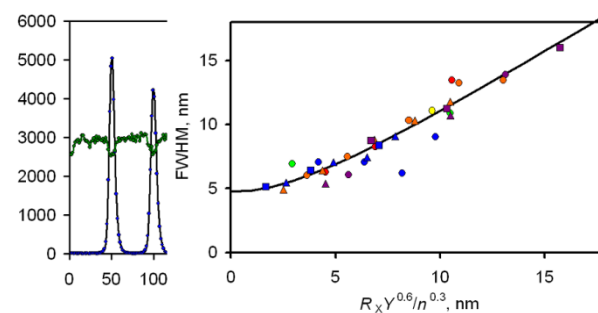


**Fig. 7** SIMS depth profile of an Irganox 1010 sample with four Irganox 3114 delta layers using 5 keV Ar<sub>2000</sub><sup>+</sup> gas cluster ions incident at 45°, (a) whole profile for the secondary ions CNO<sup>-</sup> for Irganox 3114 and (M-H)<sup>-</sup> for Irganox 1010, (b) plot of the centroid depth of the delta layers versus the centroid dose, (c) details of five of the normalised secondary ion intensities around the fourth delta layer and (d) details of the Irganox 1010 to Si interface with fitted curves based on integrated Gaussian functions which exhibit the same FWHMs. Note

that in (b) the fitting to deduce the sputtering yield is for the four delta layers (red circles); the linear dashed extensions beyond that range do not exactly go through the end points, as described in the text. The depths are defined for a constant sputtering yield deduced from the four delta layers. In (b) the green and blue squares are the surface of Irganox 1010 and Irganox 1010 to wafer interface, respectively.

## TOC graphic

The image below is a tif file resized for the TOC. Please let me know if this is not what is required.



## 20 words highlighting the novelty of the work:

This paper presents, for the first time, the different operational parameters defining the best depth resolution in SIMS organic analysis.